JOURNAL OF SOLID STATE CHEMISTRY **133,** 51–54 (1997)
ARTICLE NO. SC977315

Electronic Structure Calculations of Hexaborides and Boron Carbide

H. Ripplinger, K. Schwarz, and P. Blaha

Technische Universität Wien, Getreidemarkt 9/158, A-1060 Vienna, Austria

Received January 21, 1997; accepted February 6, 1997

The electronic structures of several CaB_6-type hexaborides and boron carbide, B_4C, are studied by the full-potential linearized-augmented plane-wave (LAPW) method within density functional theory. The hexaborides contain inter- and intraoctahedral boron–boron bonds, which under pressure decrease approximately linearly; however, the former shrinks more than the latter, consistent with Raman spectra and a simple spring constant model. The boron–boron dumbbell is stronger than the intraoctahedral bonds. For boron carbide several substitutions of the three-atom chain are simulated (BBC, BCB, CBC, CCB, and CCC). Trends in the charge distribution are analyzed and electric field gradient calculations compared to nuclear quadrupole coupling constant measurements show that B must be in the center position.

1. INTRODUCTION

In this paper we deal with electronic structure calculations carried out on a selection of boron compounds. In the CaB_6-type hexaborides we have investigated the two different boron–boron bond lengths: the inter- and intraoctahedral, denoted BB1 and BB2, respectively (Fig. 1). The shorter BB1 bond is expected to be stronger. We have investigated how these boron–boron distances change under pressure, i.e., for decreased lattice constants. In a very simple mechanical model, in which the boron network is simulated by springs representing the BB1 and BB2 bonds, but neglecting the interactions between boron and the metal atom, the ratio of force constants for BB1 and BB2 is approximated. We present a charge analysis on hexaborides with mono-, di-, tri-, and tetravalent metal atoms. Comparison of frozen phonon calculations and results of Raman spectra performed on LaB_6 conclude our survey of CaB_6-type hexaborides.

Boron carbide, B_4C, which is closely related to α-boron, consists of icosahedral B_{12} building blocks with additional chains of three atoms inserted between the B_{12} units (Fig. 2). For a long time this three-atom chain has been a crucial point in the structure determination. Within a series of model calculations based on the crystallographic data of $B_{13}C_2$ (1) we have investigated α-B_{12}, B_{12}(BCB), B_{12}(BBC), B_{12}(CBC), B_{12}(CCB), and B_{12}(CCC). For computational reasons we had to keep the B_{12} unit, neglecting any substitution with C. We have optimized the atomic positions by minimizing forces acting on the respective nuclei. A charge analysis of the nonequivalent atoms allows a better understanding of the bonding within the chain and the boron icosahedra. Finally, we present the results of EFG calculations and make a comparison with experimental NQCC data, revealing that the central position of the chain is occupied by a boron atom.

2. METHOD

One of the most accurate schemes for determining the electronic structure of solids is the full-potential linearized-augmented plane-wave (FP-LAPW) (2) method, in which the unit cell is partitioned into atomic spheres and an interstitial region. The wave functions are described with basis functions in the corresponding regions as atomic-like functions (inside the spheres) and plane waves (in the interstitial). We have used this FP-LAPW method as embodied in the WIEN95 code (3) in a scalar relativistic version without spin–orbit coupling. Exchange and correlation effects are treated within the framework of density functional theory (DFT), and we have used both the local spin density approximation (LDA) and the improved version, namely the generalized gradient approximation (GGA), which in several applications has proven to be superior to the standard LDA. We performed total energy calculations as a function of volume and computed the forces (4) acting on the nuclei to allow an effective optimization of internal coordinates. In addition we carried out frozen phonon calculations.

The electric field gradient (EFG) tensor is defined as the second derivative of the Coulomb potential at the atomic position with respect to the nuclear coordinates, and it can be directly obtained without further approximations from the total charge density of the crystal (5, 6). The EFG provides a sensitive quantity for comparisons with NQR (nuclear quadrupole resonance) measurements.

0022-4596/97 $25.00

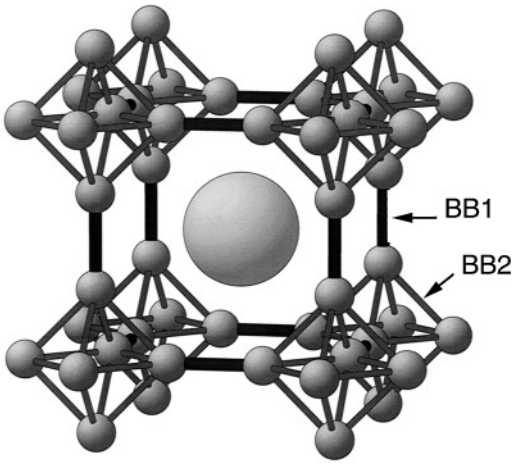

FIG. 1. CaB_6 structure showing the inter- and intraoctahedral boron–boron bonds, BB1 (dumbbell) and BB2 (octahedron), respectively.

TABLE 1
Theoretical and Experimental Lattice Constants and Interoctahedral Boron–Boron Distances (for Experimental Lattice Constants) for a Selection of CaB_6-Type Hexaborides

	Lattice constant (Å)		Interoctahedral B–B distance (Å)	
Compound	Theoretical	Experimental	Theoretical	Experimental
KB_6		4.2325	1.69[a]	
CaB_6	4.10[a]	4.1525	1.68[a]	1.68
SrB_6		4.1897	1.71[a]	
BaB_6	4.21[a]	4.269	1.75[a]	
YB_6		4.113	1.65[a]	
LaB_6	4.10[a]/4.15[b]	4.1569	1.66[a,b]	1.66
CeB_6		4.1396	1.65[a]	

Note. The experimental structure data are taken from Ref. [7] for KB_6 and from Ref. [8] for all other hexaborides.
[a] LDA.
[b] GGA.

3. RESULTS ON HEXABORIDES

Hexaborides under Pressure

As a first step we have calculated the theoretical equilibrium lattice constants (for three cases) by FP-LAPW total energy minimization and found lattice constants about 1% smaller than the experimental values when LDA was used. Although this deviation is small, it is well known to occur for LDA, whereas with GGA it leads to very good agreement with experimental data as demonstrated here for LaB_6. As a next step the interoctahedral BB1 distance of various hexaborides was calculated after fixing the volume to the experimental value. Table 1 compares these theoretical results with available experimental data (7, 8).

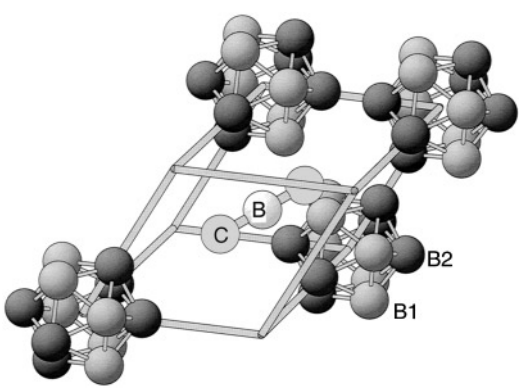

FIG. 2. Boron carbide (B_4C) and related structures consist of icosahedral B_{12} building blocks with the equatorial (B1) and axial (B2) boron atoms and the three-atom chain inserted between them. The icosahedra are linked via B2 in a rhombohedral unit cell.

These hexaborides can be considered B networks consisting of B octahedra or B dimers (dumbbell) as main building blocks, respectively. The distance within the dimers is denoted BB1 and the longer distance within the octahedra is denoted BB2 (Fig. 1). We have investigated how these BB distances vary with external pressure and found that both bond lengths decrease approximately linearly with reduced volume, but BB1 decreases more strongly than BB2 (i.e., at a 5% volume decrease BB1 and BB2 decrease by 5.5 and 4.5%, respectively). We can apply a very simple model in which each boron–boron bond is represented by a spring (with different force constants, f_{BBi}, for BB1 and BB2) while the boron–metal interactions are neglected. Considering the geometrical factors, the ratio of the force constants is then given by the relation

$$\frac{f_{\mathrm{BB1}}}{f_{\mathrm{BB2}}} = \frac{4}{1} \times \frac{\sqrt{2}}{2} \times \frac{(\Delta \mathrm{BB2}/\mathrm{BB2})}{(\Delta \mathrm{BB1}/\mathrm{BB1})},$$

where ΔBBi is the reduction of BBi with pressure. The ratio between these two force constants is 1.95 for LaB_6 and 1.90 for CaB_6. In an interpretation of Raman spectroscopic data experimentalists found for LaB_6 $f_{\mathrm{BB1}} = 2.18$ mdyne/Å and $f_{\mathrm{BB2}} = 1.28$ mdyne/Å (8, 9) and thus this ratio of 1.70 is close to our crude estimate.

Frozen Phonon Calculations

After small displacements of the atoms we can use the forces acting on the atomic nuclei to obtain the frequencies of the respective phonons, which can be compared, e.g., to Raman spectroscopy. In the hexaborides the A_{1g} phonon is

due to the breathing of the boron octahedra, the simplest vibration for computations. We obtain (using GGA) a frequency of 1218 cm^{-1} for the A_{1g} mode in LaB_6, which is in excellent agreement with the experimental result of 1245 cm^{-1} (10). The E_g phonon consists of an asymmetric breathing of the octahedra in x, y, and z directions, respectively. The resulting frequency of 1097 cm^{-1} also agrees well with the measured value of 1125 cm^{-1}.

Charge Analysis

CaB_6-type hexaborides can host mono-, di-, tri-, and tetravalent metal atoms in their three-dimensional boron network. We present here a charge analysis for KB_6; Ca-, Sr-, and BaB_6; Y- and LaB_6; and CeB_6; these represent all four cases mentioned above. The valence B charge (within the boron sphere of 0.794 Å) is displayed (in Fig. 3) as a function of the average valence electron concentration (VEC) for these compounds. (The VEC is the total number of valence electrons divided by the volume of the unit cell.) It is striking that the hexaborides of the mono- (K) and divalent (Ca, Sr, and Ba) metals fall onto a straight line, indicating a strong linear dependence of the boron charge upon the VEC. This surprising linearity indicates that VEC effectively combines different chemical quantities such as ionicity, covalency, and the size of the ions into one variable. YB_6 deviates only slightly from this linear dependence, while La- and CeB_6 show a distinct deviation. However, if we neglect the 4*f* electrons and calculate the VEC of LaB_6 and CeB_6 (i.e., and take La and Ce to be divalent ions), these charges lie close to the straight line, indicating that the 4*f* electrons are localized and thus should not be included in the VEC. The reader should note a recent LMTO study by Suvasini *et al.* (11) on the Fermi surface of CeB_6. They could not conclusively determine whether or not the 4*f* electrons were localized. In the trivalent case of YB_6, the linearity obtained suggests that the 4*d* electron only partly contributes to the VEC and is not as localized as the Ce 4*f* states.

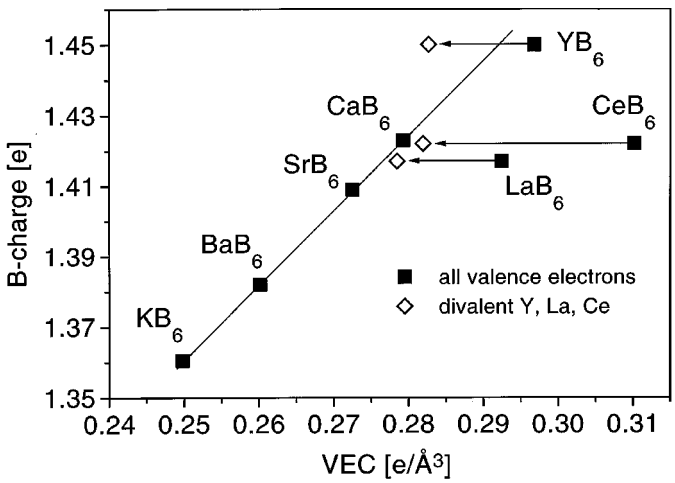

FIG. 3. Correlation between B charge and VEC, the valence electron concentration (number of valence electrons per unit cell volume). The B charge is determined as the valence charge inside the boron sphere (with $r_B = 0.794$ Å). Assuming localized 4*f* states for La and Ce or 4*d* states for Y makes these atoms divalent.

4. RESULTS ON BORON CARBIDE

Charge Analysis

We present a charge analysis of the two nonequivalent icosahedral boron atoms B1 and B2 and the two nonequivalent chain atoms designated chain B and chain C, respectively (Fig. 2). Table 2 gives *s*- and *p*-like electronic charges within the boron/carbon spheres in B_{12}(BCB), B_{12}(CBC), and B_{12}(CCC) and within the boron spheres in α-B_{12}. All atomic spheres are chosen with a radius $r =$ 0.688 Å, except for the chain atoms in B_{12}(CCC), for which $r = 0.661$ Å is taken in order to prevent the spheres from overlapping within the chain, since, according to our structure optimization, the CCC chain is remarkably shorter (length = 2.657 Å) than the BCB (2.806 Å) or CBC chain (2.878 Å). One can easily verify that the *p*-like charge of the B1 boron increases substantially due to the insertion of the chain between the boron icosahedra, while the *s*-like charge increases only slightly. The B2 boron shows only a slight increase for both *s*- and *p*-like charges. In the chain boron of B_{12}(CBC) the *s* charge (*p* charge) is significantly larger (smaller) than the corresponding values of the icosahedral boron atoms. Electronic charges in the carbon sphere are obviously higher than those in the boron spheres due to the additional valence electron.

TABLE 2

Partial *s*- and *p*-like Charges (e) for the Nonequivalent Positions of the Model Crystals α-B_{12}, B_{12}(BCB), B_{12}(CBC), and B_{12}(CCC)

	B_{12}CBC		B_{12}BCB		B_{12}CCC		α-B_{12}	
Position	*s*	*p*	*s*	*p*	*s*	*p*	*s*	*p*
B1	0.296	0.645	0.309	0.658	0.292	0.650	0.286	0.576
B2	0.299	0.629	0.304	0.631	0.297	0.638	0.295	0.624
Chain B	0.385	0.556	0.331	0.731	—	—	—	—
Chain C	0.598	1.366	0.727	1.116	0.641/ 0.551[a]	1.076/ 1.229[a]	—	—

Note. Atomic spheres are all with $r = 0.688$ Å; however, for the CCC chain due to the shorter equilibrium distances the atomic sphere radii were chosen to be $r = 0.661$ Å.

[a] The end position of the chain.

TABLE 3
EFG of Icosahedral and Chain Boron Positions in the Model Crystals B_{12}(BBC), B_{12}(BCB), B_{12}(CBC), B_{12}(CCB), B_{12}(CCC), and Experimental B_4C (Taken from Ref. 12 and Ref. Therein)

	EFG (10^{21} V/m^2)					
Position	B_{12}(BBC)	B_{12}(BCB)	B_{12}(CBC)	B_{12}(CCB)	B_{12}(CCC)	Exp. B_4C
B1	$\|EFG\| < 1.1$	0.25	− 0.69	$\|EFG\| < 0.6$	0.54	0.71–0.2
B2	$\|EFG\| < 1.6$	− 1.14	− 0.51	$\|EFG\| < 1.2$	− 1.33	1.32 ± 0.1
Chain boron	$\|EFG\| < 3.6$	− 1.21	**− 5.83**	$\|EFG\| < 1.2$	—	**5.68 ± 0.02**

Note. Data for B_{12}(BBC) and B_{12}(CCB) are upper limits for the absolute value of the EFGs.

EFG Results

Table 3 shows EFG data of the nonequivalent chain atoms of B_{12}(BBC), B_{12}(BCB), B_{12}(CBC), B_{12}(CCB), and B_{12}(CCC) and experimental data of boron carbide (B_4C). Data for B_{12}(BCB) and B_{12}(CBC) have been given in a previous paper (12), which also contains an additional analysis and interpretation of EFG results. EFGs of the boron icosahedra are highly sensitive to shifts of atomic positions and thus the good agreement between the computed EFGs of B1 and B2 EFGs for B_{12}(CCC) and the experimental B_4C should not be overemphasized. Here we focus on EFGs of the three-atom chain which are insensitive to the chain positions and are nearly independent of the positions of the icosahedral boron atoms (regarding a small deviation from equilibrium). The large value of the EFG has been associated with the central position of the chain using experimental techniques (13), and we can definitely conclude that such a high EFG value in boron carbide originates solely from the central boron atom. Boron in other positions shows substantially lower absolute EFG values, as can be seen for the chains in B_{12}(BBC) and B_{12}(CCB) and especially for the icosahedral boron atoms.

5. CONCLUSION

We have dealt with a selection of CaB_6-type hexaborides and the behavior of the hexaboride crystal under pressure. A simple mechanical model yields a ratio of force constants for intra- and interoctahedral bonds of nearly 2 and a comparison of calculated and experimental Raman frequencies in LaB_6 shows excellent agreement. The charge analysis of hexaborides with mono-, di-, tri-, and tetravalent atoms shows a linear dependence of boron valence charges with the VEC for the mono- and divalent metal atoms. The tri- and tetravalent metal atoms follow the same trend provided that the strongly localized $4f$ electrons are neglected in the VEC.

A series of boron carbide compounds is investigated using a model system, in which the B_{12} icosahedra are kept (and remain unsubstituted) but the three chain atoms are varied, changing the carbon/boron occupations. A charge analysis shows a change in the *sp* hybridization between the three-atom chain and the boron in the icosahedra. EFG calculations clearly prove that in boron carbide, boron occupies the central position in the chain. This analysis has demonstrated that the WIEN95 package is a powerful tool for structure clarification in combination with spectroscopic methods.

ACKNOWLEDGMENTS

This work was partly supported by the "Hochschuljubiläumsstiftung der Stadt Wien" and the Austrian Science Foundation (FWF Project P10847).

REFERENCES

1. A. Kirfel, A. Gupta, and G. Will, *Acta Crystallogr. Sect. B* **53,** 1052 (1979).
2. D. Singh, "Planewaves, Pseudopotentials and the LAPW Method." Kluwer, Dordrecht, The Netherlands, 1994.
3. P. Blaha, K. Schwarz, P. Dufek, and R. Augustyn, WIEN95, Technical University of Vienna, 1995. [An improved and updated Unix version of the original copyrighted WIEN-code, which was published by P. Blaha, K. Schwarz, P. I. Sorantin, and S. B. Trickey, *Comput. Phys. Commun.* **59,** 399 (1990)]
4. B. Kohler, St. Wilke, M. Scheffler, R. Kouba, and C. Ambrosch-Draxl, *Comput. Phys. Commun.* **94,** 31 (1996).
5. P. Blaha, K. Schwarz, and P. Herzig, *Phys. Rev. Lett.* **54,** 1192 (1985).
6. P. Blaha, K. Schwarz, and P. H. Dederichs, *Phys. Rev. B* **37,** 2792 (1988).
7. R. Naslain and J. Étourneau, *Compt. Rend. Acad. Sci. Ser. C* **263,** 484 (1966).
8. M. Korsukova, *in* "Proceedings, 11th International Symposium on Boron, Borides and Related Compounds, Tsukuba 1993," JJAP Series 10, p. 15, 1994.
9. M. Ishii, H. Aono, S. Muranaka, and S. Kawai, *Solid State Commun.* **20,** 437 (1976).
10. H. Scholz, W. Bauhofer, and K. Ploog, *Solid State Commun.* **18,** 1539 (1976).
11. M. B. Suvasini, G. Y. Guo, W. M. Temmerman, G. A. Gehring, and M. Biasini, *J. Phys. Condens. Matter* **8,** 7105 (1996).
12. K.Schwarz, H. Ripplinger, and P. Blaha, *Z. Naturforsch. A* **51,** 527 (1996).
13. A. H. Silver and P. J. Bray, *J. Chem. Phys.* **31,** 247 (1959).